

# Onset of the Asymptotic Regime for Finite Orders

Joe Henson<sup>\*</sup>, David Rideout<sup>†</sup>, Rafael D. Sorkin<sup>‡</sup> and Sumati Surya<sup>◦</sup>

<sup>\*</sup> University of Bristol, U.K.

<sup>†</sup> University of California, San Diego, USA

<sup>‡</sup> Perimeter Institute, Waterloo, Canada

<sup>◦</sup> Raman Research Institute, Bangalore, India

We describe a Markov-Chain-Monte-Carlo algorithm which can be used to generate naturally labeled  $n$ -element posets at random with a probability distribution of one's choice. Implementing this algorithm for the uniform distribution, we explore the approach to the asymptotic regime in which almost every poset takes on the three-layer structure described by Kleitman and Rothschild (KR). By tracking the  $n$ -dependence of several order-invariants, among them the height of the poset, we observe an oscillatory behavior which is very unlike a monotonic approach to the KR regime. Only around  $n = 40$  or so does this “finite size dance” appear to give way to a gradual crossover to asymptopia which lasts until  $n = 85$ , the largest  $n$  we have simulated.

## 1 Introduction

In the opposite regimes of small and large  $n$ , much is known about the structure of the  $n$ -orders. (By “ $n$ -order” we mean an  $n$ -element partial order or *poset*, or equivalently a finite  $T_0$  topology on  $n$  points.) On the one hand, the unlabeled  $n$ -orders (isomorphism equivalence classes of  $n$ -orders) have been constructively enumerated by machine computation for  $n \leq 16$ , and their labeled counterparts have been similarly enumerated to  $n = 18$  [1]. On the other hand, the limit of large  $n$  has been treated by Kleitman and Rothschild (KR) [2], whose theorem tells us that as  $n \rightarrow \infty$  the fraction of posets belonging to a type which we will refer to as *3-layered* tends to unity. This result yields rather complete information about the structure of a typical  $n$ -order in the asymptotic regime, including information on the sizes of the three layers, as discussed below. It implies in particular that the total number of posets of cardinality  $n$  is to leading order  $2^{n^2/4}$ , independently of whether we consider the labeled or unlabeled case.

Intermediate values of  $n$  are less well understood, however. Not only is it unknown how a typical poset is structured in this regime, but it is not even known at which value of  $n$  the asymptotic KR behaviour sets in. Of course no question like the latter can expect a precise answer. Are we in asymptopia if 90% of the  $n$ -orders are of KR type, or must it be 99.9%, or 99.99%? More importantly, any attempt to define precisely the “KR class” of posets will depend on which features one is interested in, for example

the height or the number of related pairs of elements. Herein we consider a number of such indicators, and find a relatively consistent picture emerging, of where and how the transition to asymptopia takes place.

We address this question numerically, using the technique known as Markov Chain Monte Carlo (MCMC). Our MCMC algorithm is designed to sample uniformly from the set  $\Omega_n$  of naturally labeled  $n$ -orders, where by a natural labeling we mean a labeling by natural numbers which is compatible with the partial ordering itself. (In effect, the algorithm weights a poset by the number of its linear extensions. We have found such a weighting to be particularly easy to implement numerically, and it arises naturally in the context of certain growth dynamics for causal sets [3, 4].) While a random sampling is not as definitive as an exhaustive enumeration, it does provide important evidence on the structure of  $\Omega_n$ , producing some surprising (or at least, as far as we know, unanticipated) results.

By design, our Markov dynamics satisfies ergodicity and detailed balance, but that alone would only guarantee the desired sampling probabilities in the unrealizable limit of an infinitely long run (and provided we had a perfect random number generator). To assess whether a uniform sampling has in fact been achieved, we have run our Markov process with widely different initial posets, finding excellent evidence that thermalization occurs on practical time-scales for  $n \leq 85$ . Agreement with known exact results for  $n = 9$  provides a further reason for confidence in our simulations.

A 3-layered poset has a height of three (or less depending on the precise definition one adopts), and height thus provides one possible indicator of when the asymptotic regime has been reached. Judged on this indicator, our simulations exhibit a surprisingly colorful behavior which lasts until  $n \approx 45$ , and only then appears to switch over to a gradual approach to the asymptotic limit. To be more precise, the measured fraction of posets of height 3 actually *decreases* for  $7 \leq n \leq 30$ , falling below 3% at  $n = 30$ . At this point, however, it initiates a slow increase, such that the height 3 posets make up over 90% of the total for  $n \geq 80$ .

Similar results are obtained for other indicators of KR-like behavior, including the possession of a layered structure, the cardinalities of the levels (to be defined below), and the total number of relations. Taken as a whole, the evidence from our simulations suggests a gradual crossover to asymptopia which begins around  $n = 43$ , and is still in progress at  $n = 85$ , the largest value we have simulated. At what point one could say with confidence that one had unequivocally entered the asymptotic regime is difficult to assess from our data, but it looks to be at least  $n = 100$  or greater.

The development of a reliable MCMC technique for posets is a uniquely challenging problem that

(in comparison with the Ising model for example) will probably require qualitatively new methods for its solution. The need to maintain the very nonlocal constraint of transitivity presents novel difficulties because it introduces a highly “inseparable” mutual dependence among the relations defining the poset; and as far as we are aware simulations of the uniform distribution on  $\Omega_n$  have not been attempted until now (although see [5] for a similar application of MCMC techniques). On this first attempt, we have found our MCMC scheme to be practical up to  $n = 85$ , or for a perhaps fairer comparison with other simulations, up to 3321 possible relations. This offers hope that larger values of  $n$  could be accessed by further technical developments.

One of our main reasons for developing the techniques presented in this paper comes from the poset’s potential role in quantum gravity, and specifically from its role in the theory of causal sets. The point-events of a spacetime which is free of causal pathologies<sup>1</sup> are partially ordered by the relativistic light-cone structure. This is a key motivation for the causal set programme, which substitutes for the spacetime continuum a locally finite partially ordered set [6]. Such a poset thus represents a possible causal structure, and one can regard a natural labeling thereof as a possible “birth order” of its elements. We expect the techniques and results presented herein to be relevant to the study of non-uniform measures on  $\Omega_n$ , such as arise [7] in attempts to devise a quantum-gravity theory based upon the dynamics of the discrete causal structures we have just described.

## 2 Initial considerations

### 2.1 Definitions

A partially ordered set or *poset* is determined by a pair  $(S, \prec)$ , where  $S$  (also called the *ground set*) is a set and  $\prec$  is a binary relation on  $S$  which is transitive ( $x \prec y \prec z \implies x \prec z \forall x, y, z \in S$ ) and (in our convention) irreflexive ( $x \not\prec x \forall x \in S$ ). When  $x \prec y$ , we will sometimes express this by saying that  $x$  “precedes”  $y$  or  $y$  “follows”  $x$ . We will consider for our simulations only posets on the finite set  $S = [n]$ , where  $[n] = \{0, 1, 2, \dots, n-1\}$ , and all of our posets will be *naturally labeled*, in the sense that  $x \prec y \implies x < y, \forall x, y \in [n]$ . We will refer this set of posets as the *sample space* and denote it as  $\Omega_n$ . An isomorphism equivalence class of posets will be called an *unlabeled poset*.

By an *order invariant* or *observable* of a poset  $S$  we will refer to a property that is invariant under isomorphisms, or in other words is independent of the labeling, natural or otherwise. We will now define a set of such invariants which will be employed in the remainder of the paper. An *antichain* is a subset of

---

<sup>1</sup>technically, a time-oriented Lorentzian geometry which contains no closed causal curve

$S$  among whose elements there are no relations  $\prec$ . A *chain* is a subset of  $S$ , every pair of whose elements is related by  $\prec$ , and the *length* of a chain is its cardinality. The *height* of a poset is the length of the longest chain that it contains. A *minimal element* of  $S$  is one with no element of  $S$  preceding it, while a *maximal element* has no element following it. A *link* is a relation  $x \prec y$  which is not implied by other relations via transitivity, i.e.,  $x \prec y$  and  $\nexists z$  such that  $x \prec z \prec y$ . The total numbers of links  $L$  and relations  $R$  in a given poset offer other useful invariants. We define the *linking fraction*  $l = 4L/n^2$  or  $4L/(n^2 - 1)$  for  $n$  even or odd, respectively, and the *ordering fraction*  $r = R/\binom{n}{2}$ , whose denominator is the total number of possible relations on  $n$  elements. The *past* of an element  $x$  consists of those elements which precede it in the order:  $\text{past}(x) = \{z : z \prec x\}$ . The *inclusive past* of  $x$  includes  $x$  as well,  $\text{incpast}(x) = \text{past}(x) \cup \{x\}$ . Likewise we define the *future* and *inclusive future* as  $\text{fut}(x) = \{z : x \prec z\}$  and  $\text{incfut}(x) = \text{fut}(x) \cup \{x\}$ . For  $x \prec y$  the *interval*  $I(x, y) = \text{fut}(x) \cap \text{past}(y)$ . Counting, for each  $k$ , the number of intervals of cardinality  $k$  produces another set of invariants containing a large amount of information about the structure of the poset.

One can recursively partition a poset into *levels*  $L_1, L_2, \dots, L_k$  as follows. An element  $x \in L_1$  if  $\text{past}(x) = \emptyset$ , otherwise  $x \in L_n$  if the maximum value of  $m$  for which there exists  $y \prec x$  with  $y \in L_m$  is  $n - 1$ . Equivalently,  $n$  is the cardinality of the longest chain terminating at  $x$ .

## 2.2 The Kleitman-Rothschild theorem

The Kleitman-Rothschild theorem offers a precise answer to the question of what a typical poset looks like in the limit of large  $n$ . We state it in essentially the same form as Brightwell [8], making use of the following families of “layered” posets. Consider disjoint sets  $X_1, X_2, \dots, X_k$  of elements, and let  $\mathcal{A}(X_1, X_2, \dots, X_k)$  denote the set of partial orders definable on  $\cup_{i=1}^k X_i$  such that

- (1) if  $x \in X_i, y \in X_j$ , and  $x \prec y$ , then  $i < j$ , and
- (2) if  $x \in X_i, y \in X_j$ , and  $i < j - 1$ , then  $x \prec y$ .

Note that each  $X_i$  forms an antichain, which we call *layer*  $i$ . For any poset whatsoever, its partition into *levels* clearly fulfills condition (1), but not necessarily (2). Finite posets in the class  $\mathcal{A}(X_1, X_2, \dots, X_k)$  have a number of readily deduced properties, the most obvious of which is that they have height  $\leq k$ .

We will say that *in the limit of large  $n$ , almost every poset* has a certain property if, as  $n \rightarrow \infty$ , the fraction of posets lacking that property goes to 0. We will also say that the posets with such a property *dominate at large  $n$* .

**KR theorem:** Let  $\omega(n)$  be any function tending to infinity. In the limit of large  $n$ , almost every partial order with ground-set  $[n]$  lies in the class  $\mathcal{A}(X_1, X_2, X_3)$  for some partition  $(X_1, X_2, X_3)$  of  $[n]$  such that  $||X_2| - n/2| < \omega(n)$ ,  $||X_1| - n/4| < \omega(n)\sqrt{n}$ , and  $||X_3| - n/4| < \omega(n)\sqrt{n}$ .

The above theorem informs us that asymptotically almost every  $n$ -order is a *three-layer poset* in the sense that it belongs to the class  $\mathcal{A}(X_1, X_2, X_3)$ , and from this follow other asymptotic properties not stated explicitly in the theorem. Such properties are often easy to derive, if one notices that in the uniform random distribution of posets in  $\mathcal{A}(X_1, X_2, X_3)$ , each random variable associated to the existence of a relation between elements in  $X_1$  and  $X_2$ , or between  $X_2$  and  $X_3$ , is independent. For example, one can prove in this way that the posets of height 3 dominate at large  $n$ . This is not true tautologically, because our definition of a layered order allows any of the three layers to be empty, and because condition (2) above does not force an element in layer 2 to be related to any other element in layer 1 or 3. Nonetheless, in view of the previous observation, it is not difficult to see that the fraction of 3-layer posets of height  $< 3$  tends to 0 as  $n \rightarrow \infty$ . By similar reasoning it is not hard to demonstrate that, for the uniform distribution over 3-layer orders, the ordering fraction is concentrated near to  $r = 3/8$ . From the theorem as stated, one can also derive, by counting the possible 3-layer orders, that the total number of  $n$ -orders grows as  $2^{n^2/4}$ , up to a subdominant supplementary factor. All of these properties can be regarded as characteristic of the asymptotic regime.

The  $n$ -orders referred to in the KR theorem as stated above are “arbitrarily labeled posets”, *i.e.* posets on  $[n]$  with no further restrictions. Although the set of all such posets will obviously differ from the set of unlabeled  $n$ -orders, Kleitman and Rothschild showed that their result holds for unlabeled orders as well. Intuitively, a labeling can introduce a factor of at most  $n!$ , and  $n!$ , imposing as it might seem, is subdominant compared to  $2^{n^2/4}$ . (In this connection, it’s worth emphasizing that for large  $n$ , almost every 3-layer  $n$ -order is asymmetric: it admits no nontrivial automorphism.)

As mentioned, however, our simulations produce neither unlabeled nor arbitrarily labeled posets, but naturally labeled ones, a choice which allows for efficient machine representation of a poset as an upper-triangular matrix.<sup>2</sup> In comparison with a uniform weighting over unlabeled  $n$ -orders, our sample-space thus weights each unlabeled poset by the number of its linear extensions (or more precisely by the number of inequivalent linear extensions, where two linear extensions are equivalent iff they are related by an automorphism of the poset).

---

<sup>2</sup>An upper-triangular bit-matrix  $M$  defines a binary relation on  $[n]$  via the rule  $j < k \iff M_{jk} = 1$ . If one adds the condition of transitivity, then  $M$  yields a general element of  $\Omega_n$ .

Insofar as one cares only about enumerating the  $n$ -orders asymptotically, the distinctions among unlabeled, naturally labeled, and arbitrarily labeled posets can (as just explained) be ignored, unless one is interested in the subleading terms: the resulting under- or over-counting could “at most” introduce a factor of  $n!$ . However, the KR theorem, in the form given above, also says something about the typical sizes of the three layers, and here the choice of natural labeling will make a difference, because a reallocation of poset elements between the top and bottom layers has no effect on the leading order counting. A closer analysis, based on an estimate we reproduce in the Appendix, leads us to expect that the size of the bottom (or top) layer is more likely to vary uniformly between 0 and  $n/2$  than to be concentrated near  $n/4$  as the KR theorem would have it. And this in turn would imply a less concentrated asymptotic ordering-fraction averaging to  $1/3$  instead of  $3/8$ . (Asymptotically  $r$  would be distributed between  $1/4$  and  $3/8$  with a square-root-divergent peak at  $3/8$ , which accordingly would still be its “most likely value”.)

Finally, let us comment that the choice of natural labeling can also be motivated by its application to the physics of spacetime, and specifically by the example of “sequential growth dynamics” in causal set theory. In that context a measure is defined on the space of countable posets corresponding to a certain Markov process, wherein the labels acquire a temporal meaning [3, 4, 9, 10].

### 2.3 In search of the asymptotic regime

As stipulated earlier, the question of where the asymptotic regime begins is inherently ambiguous, but if we don’t demand too much quantitative precision, we can come up with some reasonably natural criteria. The question amounts to deciding what should count as a “KR order”, and then asking at what value of  $n$  the majority of  $n$ -orders are in fact of this form.

The theorem quoted above suggests first of all that one should define a KR order to be 3-layered (albeit even this is subject to some doubt, as the definition given above is only one of several possible variations on the same theme). The theorem also limits the sizes of the three layers, but unfortunately it does so in a manner that tends to lose its meaning when applied to a definite, finite  $n$ . (Whether or not any given poset satisfies  $||X_2| - n/2| < \omega(n)$  depends entirely on what choice we make of the arbitrary function  $\omega(n)$ .) What remains is the semi-quantitative criterion that the middle layer should hold about half the elements, with the other two layers each holding around a fourth (albeit with larger fluctuations than for the middle layer). We have seen, however, that the condition on the top and bottom layers is inappropriate when the sample space consists of naturally labeled orders, as it does for us. Instead we

expect something more like a uniform distribution of sizes for those layers. Further natural criteria we have encountered are that the height should be exactly 3 and that the ordering fraction  $r$  should take on a characteristic value, plausibly varying between  $1/4$  and  $3/8$  with a mean of  $1/3$ . In the following, we explore all these criteria.

### 3 The Markov chain

The canonical application of the MCMC technique concerns a collection of  $\mathbb{Z}_2$ -valued “spin” variables on a regular lattice, where the probability distribution one is attempting to simulate is given by an easily computed “Boltzmann weight”. Two features that make such models easy to deal with are that (a) the configurations are expressible in terms of a fixed set of independent variables simply related to the Boltzmann weight, and (b) there are available obvious “local Monte Carlo moves” that need only refer to an easily defined, small region of the overall configuration, e.g. “flipping” one of the spins. Not all successful MCMC simulations have relied on property (a), for instance one has simulated ensembles of simplicial manifolds (see e.g. [11]) but in the case of posets even property (b) is lacking. As a result, efficient moves seem to become increasingly hard to devise as  $n$  increases.

In [5] MCMC methods were used to study the space  $\Omega_n^{2d}$  of  $n$ -element two dimensional orders, which is a proper subset of  $\Omega_n$ . The asymptotic limit for the uniform distribution on 2d orders was found by Winkler and El Sauer [12, 13], and an analogous question about onset of the asymptotic regime could be asked in that case. The results of [5] indicate that the asymptotic regime is realized for  $n$  as small as 30. However, 2d orders are structurally very different from generic posets, and it would be no surprise if the onset of asymptotic behavior took on a different character in the two cases. Notice also that features (a) and (b) are both present for 2d orders, so that one learns from them little about the process of equilibration which could be applied to the full  $\Omega_n$ .

The Markov chain on  $\Omega_n$  which we used in the present work employs a mixture of *relation moves* and *link moves*, as described in detail below. Roughly, one removes or adds a relation or a link (as defined above) between a pair of randomly chosen elements of the poset. The simulations reported herein used a uniform mixture of the two types of moves. Each type was tried in independent trials and it was found that thermalization was substantially hastened when both types were employed together.<sup>3</sup>

In order that a Markov chain on some sample-space of “states” converge to the desired equilibrium

---

<sup>3</sup>We also experimented with a third move inspired by the dynamics of “transitive percolation” [3]. However it did not seem to speed up the thermalization of the Markov chain.

distribution, it suffices that the moves it employs be ergodic and that their conditional probabilities be chosen to satisfy detailed balance [14]. Ergodicity merely requires that it be possible to pass (with non-zero probability) from any state to any other state. Detailed balance is the condition that

$$\Pr(A) \Pr(A \rightarrow B) = \Pr(B) \Pr(B \rightarrow A), \quad (1)$$

where  $A$  and  $B$  are any two states,  $\Pr(X)$  is the desired probability of state  $X$ , and  $\Pr(X \rightarrow Y)$  is the transition-probability from  $X$  to  $Y$  that one specifies in setting up the Markov chain. Since in our case we seek the uniform distribution over states (i.e. posets in  $\Omega_n$ ), we need only ensure that each move has the same transition probability as its inverse. (We remark here that while ergodicity is trivially necessary for the desired equilibrium, detailed balance is only a matter of choice. Other conditions would serve as well, and in certain situations they might be more efficient.)

By a uniform mixture of relation- and link-moves we simply mean that at each step we flip a fair coin and propose one or the other type of move with equal probability. If the transition probabilities for the two move-types are given by  $\Pr_r$  and  $\Pr_l$ , then detailed balance for an equal mixture of the two types plainly requires that

$$\Pr_r(A \rightarrow B) + \Pr_l(A \rightarrow B) = \Pr_r(B \rightarrow A) + \Pr_l(B \rightarrow A), \quad (2)$$

a condition which is clearly satisfied if each move individually satisfies its own detailed balance condition (1). Likewise, a mixture of two ergodic move types is a fortiori ergodic.

In order to describe the relation and link moves fully we will, for the remainder of this section, think of the elements of our  $n$ -order as being the natural numbers from 0 to  $n - 1$ . (Thus each element serves as its own label.) On the computer we represent a labeled partial order by its so-called adjacency matrix  $A$ , defined by:  $A_{ij} = 1$  iff  $i \prec j$ , otherwise 0. Irreflexivity then sets the diagonal of  $A$  to zero, while the labeling is natural iff  $A$  is upper triangular.

We will need two more definitions in order to describe our moves. A *critical pair* is a pair of elements  $x < y, x \not\prec y$  for which  $\text{past}(x) \subseteq \text{past}(y)$  and  $\text{fut}(y) \subseteq \text{fut}(x)$ . A *suitable pair* is a pair of elements  $x < y, x \not\prec y$ , such that there exists no  $z \in \text{incpast}(x)$  which is linked to an element  $w \in \text{incfut}(y)$ .

The *relation move* is:

1. Select a pair of elements  $x < y$  uniformly at random.
2. If  $x$  and  $y$  are linked, remove the single relation  $x \prec y$ .

3. Else if  $x$  and  $y$  form a critical pair, adjoin the single relation  $x \prec y$ .
4. Otherwise leave the poset unchanged.

Since a succession of relation-moves can clearly transform any poset to (say) a chain, they can transform any poset to any other, hence this move is ergodic. Moreover, it satisfies detailed balance: Consider first a linked pair  $(x,y)$  whose relation  $x \prec y$  gets removed. The probability to select the pair is  $\frac{2}{n(n-1)}$ , while the probability to accept the move is 1. After the move is completed  $(x,y)$  will be a critical pair. The inverse of this move begins with a critical pair  $(x,y)$  and adjoins the relation  $x \prec y$ . The pair  $(x,y)$  is selected with the same probability  $\frac{2}{n(n-1)}$ , and the move is accepted with probability 1. After the move is completed  $(x,y)$  will be a linked pair. In the event that the selected pair forms neither a link nor a critical pair, the poset does not change. In this case the move is its own inverse, and “both” trivially share the same probability.

The *link move* is:

1. Select a pair of elements  $x < y$  uniformly at random.
2. If  $x$  and  $y$  are linked
  - (a) Remove all relations between elements of  $\text{inccast}(x)$  and elements of  $\text{inccut}(y)$ .
  - (b) Restore every relation which is implied by transitivity (via an element which is unrelated to at least one of  $x$  or  $y$ .)
3. Else if  $x$  and  $y$  form a suitable pair, adjoin a relation  $x' \prec y'$  for every pair of elements  $x' \in \text{inccast}(x)$  and  $y' \in \text{inccut}(y)$ .
4. Otherwise leave the poset unchanged.

If this description seems a bit complicated, it is because a link move acts directly, not on the adjacency matrix but on the “link matrix”. That is it effectively acts on the poset construed as a set of *links* rather than as a set of *relations*. Pictorially, it inserts or deletes an edge in the Hasse diagram of the poset, which is a directed graph containing an edge for every linked pair of poset-elements. Since such diagrams are in one to one correspondence with partial orders, it is clear that the link move is ergodic. (One can convert any poset to an antichain by removing all of its links.) Detailed balance is satisfied much in the same way as for the relation move. The selection probability is  $\frac{2}{n(n-1)}$  for each potential move from a given poset. Each potential move either leaves the poset unchanged, or converts it to a different poset with probability

1. In the latter case, the inverse move, which is the only way to return to the original poset, has the same selection and acceptance probability as the original move. Thus detailed balance is satisfied.

Note that a relation added between a critical pair creates no further new relations, and likewise a link inserted between a suitable pair creates no further links. (In fact, we could have taken this as the definitions of such pairs.) For this reason, the matching inverse moves are easy to identify as simply deleting the relation or link that was added.

## 4 Code details

We have implemented the above Markov chain Monte Carlo algorithm as a module within the Cactus high performance computing framework [15], making use of the `CausalSets` toolkit (some details are available in [16]). The `CausalSets` toolkit provides basic infrastructure for working with partial orders, including data structures and numerous algorithms needed to implement the above moves and compute order invariant ‘observables’.

We compute pseudo-random numbers using the maximally equidistributed combined Tausworthe generator of L’Ecuyer [17], as implemented in the GNU Scientific Library [18].

For a given value of  $n$ , we generally start the Markov chain with four different starting posets, to aid in determining when it thermalizes. The starting posets are a chain, antichain, a random Kleitman-Rothschild order (with  $\lfloor n/2 \rfloor$  elements in the middle layer, the cardinality of the bottom layer selected from a Poisson distribution with mean  $\lfloor n/4 \rfloor$ , and the remaining elements going into the top layer), and a bipartite order from  $\mathcal{A}(X_1, X_2)$  with  $|X_1| = \lfloor n/2 \rfloor$  and every element of  $X_1$  related to every element of  $X_2$ . We then execute a large number of sweeps (the exact number depending upon  $n$ ), where each sweep consists of  $2n^3$  attempted moves. At the end of each sweep we record a large number of observables including height, ordering fraction, and numbers of minimal and maximal elements. We regard attempted moves which change the poset as ‘accepted’, and others as ‘rejected’. Each move has an acceptance rate close to  $1/2$  for all the simulations that we have performed. Note that our choice of  $2n^3$  attempted moves per sweep is longer than the more natural choice of  $\binom{n}{2}$  attempted moves, the number needed so that on average each relation is visited once per sweep. We found, however, that sampling (and then storing) the observables as often as this consumed a great deal of disk space, making sweeps of length  $2n^3$  more practical. (In fact, for  $n \geq 69$ , the autocorrelation times are long enough that sweeps of length  $2n^5$  are justified.)

The results come from many core-years of compute time, both on the Lonestar cluster at the Texas

Advanced Computing Center (TACC), and a 12 core Intel Xeon X5690 workstation. In addition, extensive preliminary investigations with the link move were done on the HPC cluster at the Raman Research Institute.

Each realization of the Markov chain begins with a transient portion which must be discarded because the probabilities have not yet reached their equilibrium values. They have not yet “thermalized”, as one says. In deciding how long to wait, we employ as indicators the number of minimal elements  $N_{\min}$  and the ordering fraction  $r$ , as these two observables seem to be particularly sensitive to the approach to equilibrium. We regard the Markov chain as having thermalized when the traces of these observables versus sweep behave similarly from all four starting posets. Examples of traces of  $N_{\min}$  and  $r$  vs. sweep are depicted in Figures 1 and 2. These two observables reach equilibrium more slowly than others, such

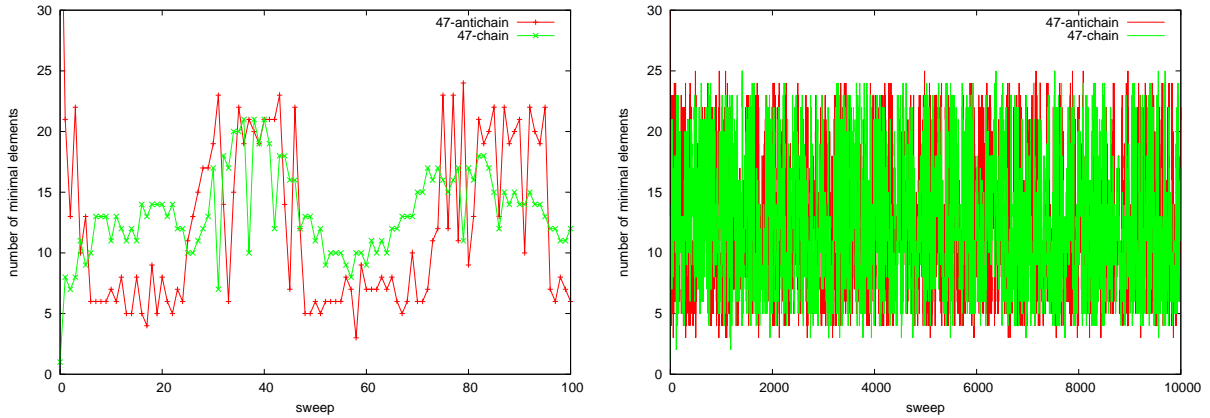


Figure 1: Trace of number of minimal elements for  $n = 47$ , starting from an antichain (red) and a chain (green). The Markov chain appears to be approaching equilibrium after 30 sweeps (if not sooner).

as the linking fraction, which appears thermalized even when the Markov chain is far from equilibrium. This can be observed by comparing with, for example, the number of minimal elements, as demonstrated in Figure 3.

After discarding the initial, unthermalized region, we estimate the autocorrelation time  $\tau$  in equilibrium, by fitting, for our various observables  $O$ , the correlator,  $\langle(O(s) - \langle O \rangle)(O(s+t) - \langle O \rangle)\rangle$  (where  $\langle O \rangle$  is the value of  $O$  averaged over all the measurements), as a function of lag-time  $t$  against an exponential curve,  $a \exp(-t/\tau)$ . Sample fits for  $n = 67$  are shown in Figure 4.

Figure 5 plots our estimates for thermalization time  $T_{\text{therm}}$  and autocorrelation time  $\tau$ , measured in sweeps. Each appears to grow exponentially with  $n$ . We performed this analysis for a limited set  $\Phi$  of poset sizes  $n$ , as illustrated in the figure. In our simulations, however, we needed to know the

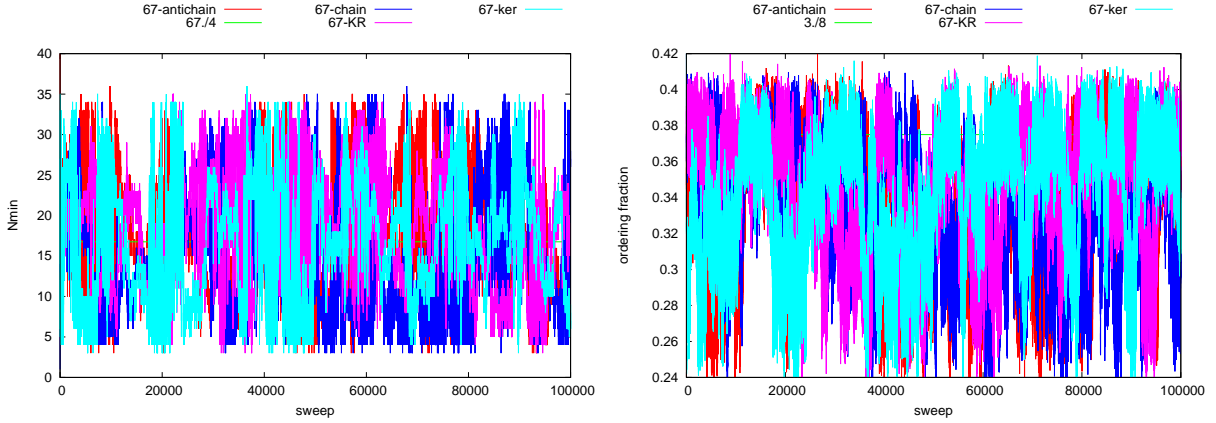


Figure 2: Trace of number of minimal elements (left) and the ordering fraction (right) for  $n = 67$ , starting from an antichain (red), a chain (blue), a Kleitman-Rothschild order (magenta), and a bipartite order with linking fraction 1 (cyan). The expected number of minimal elements for a Kleitman-Rothschild poset is  $n/4$ . The Markov chain appears to have thermalized after 41,000 sweeps.

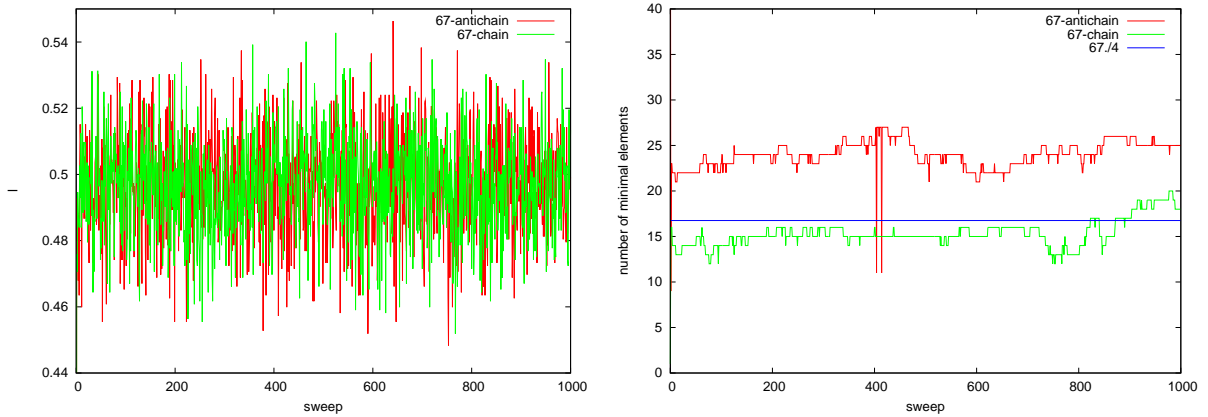


Figure 3: Trace of linking fraction (left) and number of minimal elements (right) for the first 1000 sweeps at  $n = 67$ , starting from an antichain (red) and a chain (green). By way of comparison, the thermalization time deduced from our other indicators is actually  $T_{\text{therm}} = 47,000$  for  $n = 67$ . The expected linking fraction for a Kleitman-Rothschild poset is  $1/2$ .

thermalization time  $T_{\text{therm}}$  for every  $n$  that we simulated, not only for those  $n$  in  $\Phi$ . For simplicity in such cases, we estimated  $T_{\text{therm}}(n)$  conservatively from  $T_{\text{therm}}(n_0)$  for the smallest  $n_0 \in \Phi$  such that  $n_0 \geq n$ , given the natural assumption that thermalization times increase with  $n$ .

Equipped with a thermalization time  $T_{\text{therm}}$  and autocorrelation time  $\tau$ , we compute histograms of a number of order-invariants such as height and number of relations, as follows. The simulation outputs a sequence of observable values after each sweep. We discard  $T_{\text{therm}}$  sweeps, and use the remaining samples (taken at every  $5\tau/2$  sweeps for  $n > 40$ , and at every sweep otherwise) to calculate the mean and its error.

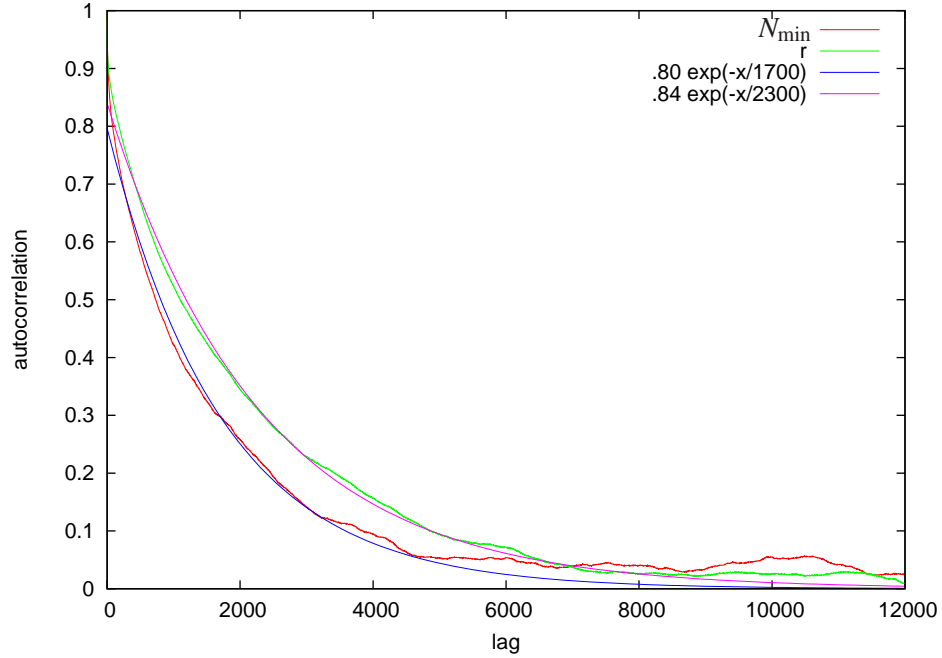


Figure 4: Autocorrelation functions of number of minimal elements (red) and ordering fraction (green) for  $n = 67$ , fitted with exponential curves in order to measure the autocorrelation time in equilibrium. Here we used  $T_{\text{therm}} = 47,000$ .

Much of our subsequent analysis is based on histograms built from these samples. We estimate each bin frequency  $f$  by the number of events which fall into that bin divided by the total number of samples  $T$ , and we estimate the statistical error in this frequency as  $\sqrt{f(1-f)/(T-1)}$ . Experimentation indicates that the resulting error estimates adequately reflect the uncertainty in the measured histogram bin frequencies. Alternatively, one could sample the time series more frequently, and use either the bootstrap or jackknife method to estimate the bin frequencies and their errors

## 5 Correctness

One of us (RDS) has generated a library of the unlabeled posets of nine or fewer elements, and has counted the natural labellings for each of them (details will appear separately [19]). We use this collection to check that our code is giving correct results.

Figure 6 compares MCMC measurements of the number of relations for 9-element posets against exact counts taken from the poset library. The left graph separately tests the relation and link moves, while the right tests a uniform mixture of both. In each case the measurements yield the correct values to within the estimated errors. Notice that using 10k samples only allows us to measure frequencies

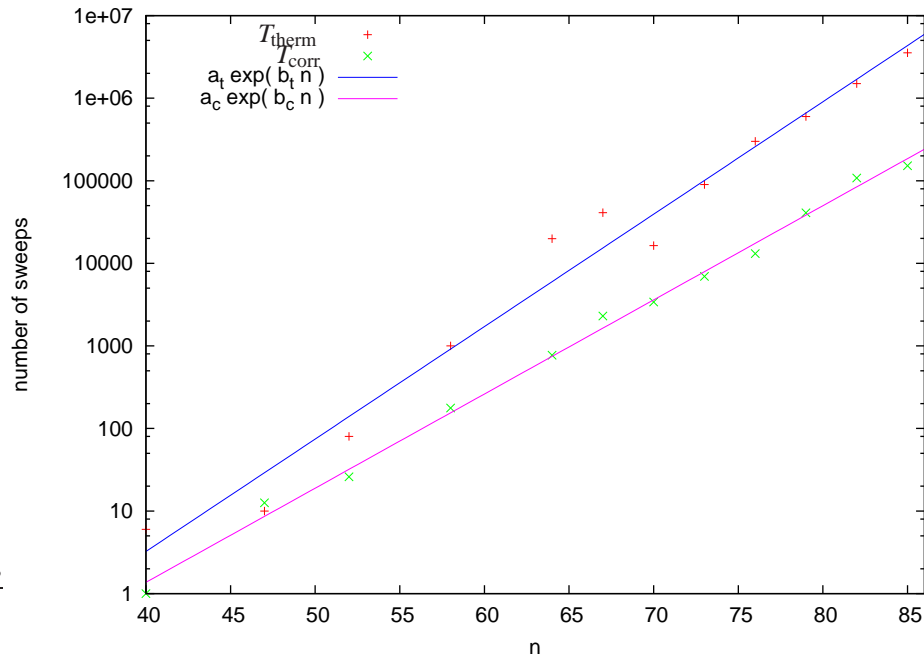


Figure 5: Measured values of thermalization time  $T_{\text{therm}}$  and autocorrelation time  $T_{\text{corr}}$  for various poset sizes  $n$ . For  $n < 40$  the autocorrelation time appears to be less than a single sweep. The best fitting exponential functions,  $T_{\text{therm}} = a_t \exp(b_t n)$  and  $\tau = a_c \exp(b_c n)$ , have  $\ln a_t = -11.4 \pm 1.0$ ,  $b_t = 0.314 \pm 0.015$ ,  $\ln a_c = -10.2 \pm .4$ , and  $b_c = 0.263 \pm .005$ .

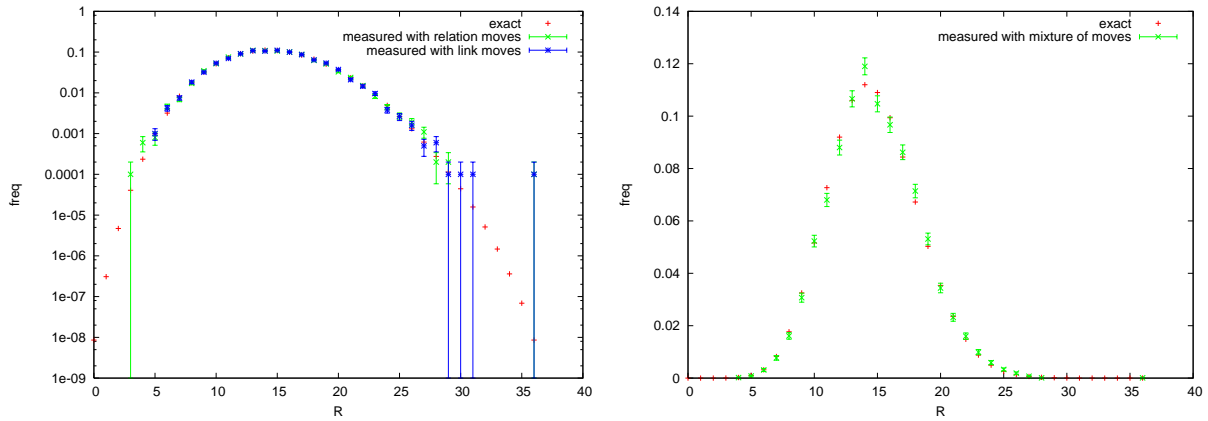


Figure 6: Checking our code against numbers of relations for (naturally labeled) 9-orders. The green and blue data comes from 10k samples, the red is exact. (Logarithmic scale on left, linear on right.)

down to  $10^{-4}$ . (The data-point with  $R = 36 = \binom{9}{2}$  represents the 9-chain that was used as the starting configuration.) Figure 7 compares MCMC measurements of the heights of 9-element posets against exact

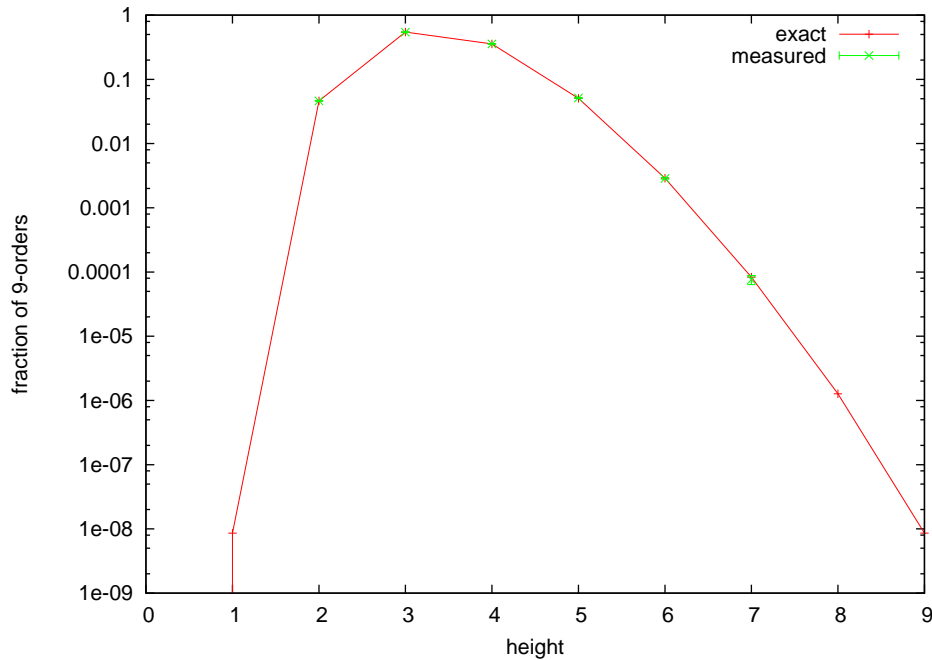


Figure 7: Heights of 9-orders measured from 10k samples (green) compared with exact values (red). (Logarithmic scale on vertical axis.)

counts from the library. Again the results match to within the error estimates. Notice that since there are fewer possible heights than relations, the measurements are more accurate. Of course, an MCMC measurement with 10k samples is still not able to resolve frequencies  $< 10^{-4}$ .



Figure 8: Sample 82 element poset.

## 6 Results

How large must  $n$  be for the asymptotic regime described by Kleitman and Rothschild to set in? As discussed in section 2.3, we address this question by measuring a number of order-invariants which take on characteristic values in the KR regime, and which therefore can herald the onset of this regime. Among these are the height, the ordering fraction  $r$ , and the property of being “layered” (especially the “connectedness” expressed by condition (2) in section 2.2). We also present results on the cardinalities of level 2 and of the minimal and maximal antichains.

We begin with a typical poset drawn from our uniform sampling at  $n = 82$ , almost the largest cardinality we have attempted to simulate. Figure 8 is the Hasse diagram of one such sample. One sees that the height is 3, and that the middle layer contains 42 elements, exactly as one would expect for an asymptotic Kleitman-Rothschild poset. By way of comparison, we show in Figure 9 a sample poset on 20 elements. It clearly does not belong to the class  $\mathcal{A}(X_1, X_2, X_3)$  of the KR theorem of Section 2.2 (nor to  $\mathcal{A}(X_1, X_2, X_3, X_4)$ <sup>4</sup>).

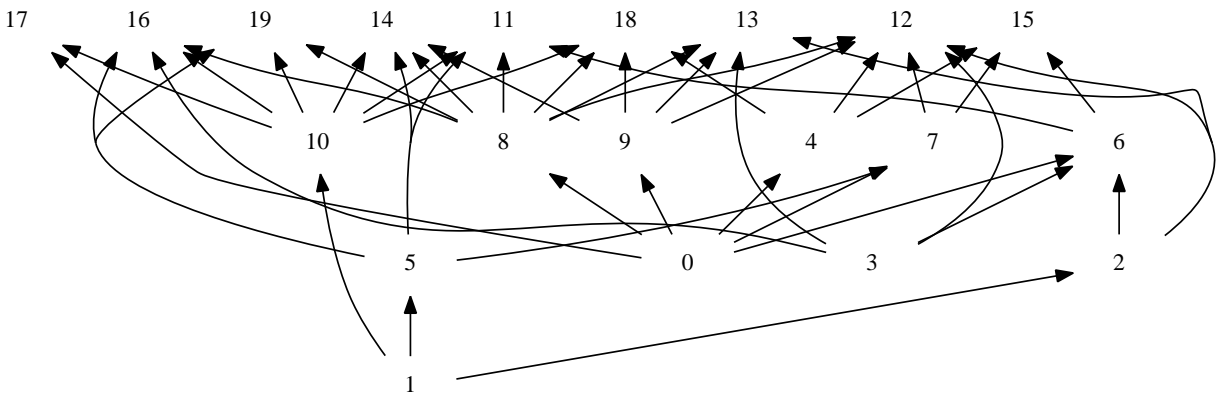


Figure 9: Sample 20 element poset.

### 6.1 Height

As we have seen, the KR theorem implies that posets of height 3 dominate as  $n \rightarrow \infty$ . Figure 10 portrays

<sup>4</sup> $1 \prec 2 \prec 6 \prec 15$ , so each would have to lie in the corresponding layer  $X_i$ ,  $i = 1 \dots 4$ . However  $2 \not\prec 18$ , which violates condition (2).

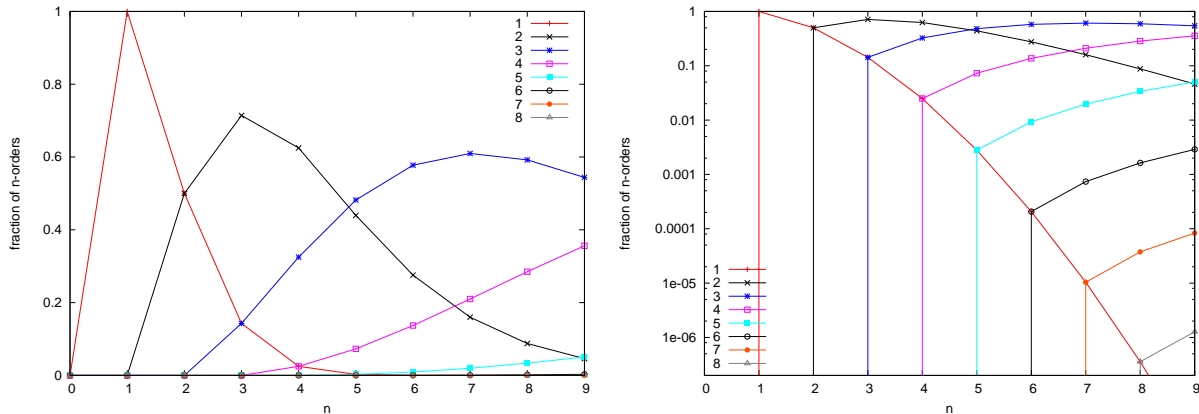
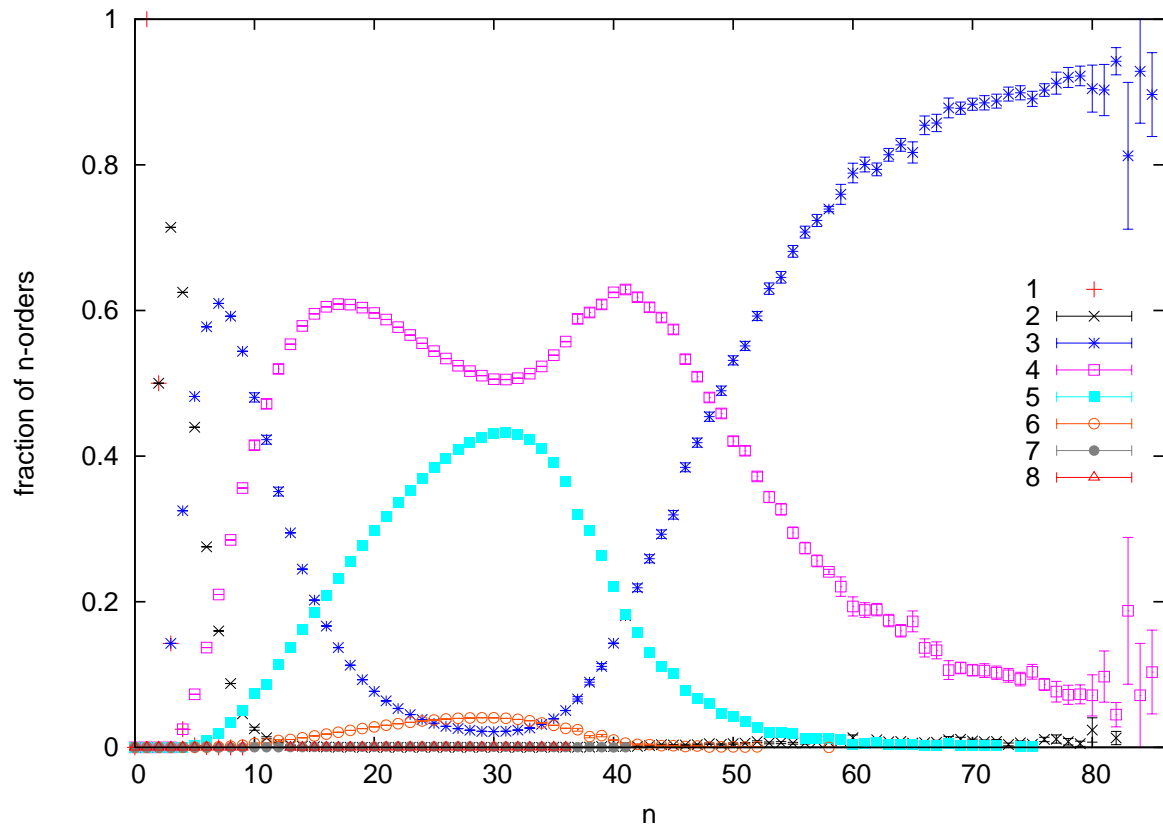


Figure 10: The exact fractions of  $n$ -orders with heights  $h = 1 \dots 9$  as a function of  $n$  for  $n \leq 9$ . (Linear scale on the left, logarithmic on the right.)

what we know from exact computations [19] of the heights of posets with  $n \leq 9$ . The fraction of naturally labeled posets with height  $h = 1 \dots 9$  is plotted as a function of  $n$ . One observes that while  $n$ -orders with height=3 are indeed in the majority for  $n > 5$ , their relative abundance begins to decrease at  $n = 7$ , while the corresponding curves for heights  $h \geq 4$  are all growing. (This can be seen most clearly in the logarithmic plot on the right of figure 10.) This indicates that, by any reasonable standard,  $n = 9$  is *not* in the asymptotic regime.

Our simulations now allow us to supplement these exact results with statistical ones for  $n \leq 85$ . We display our results in Figures 11 and 12, which extend Figure 10 out to  $n = 85$ . It is evident that the departure from KR-like behavior which started to show up in the exact data continues for  $n > 9$  and becomes most pronounced around  $n = 30$ . The curves for  $h \leq 3$  peak at small  $n \leq 7$ , and then diminish rapidly as the  $n \approx 30$  region is approached, whereas the height fractions for  $h \geq 5$  all reach their maxima at  $n \approx 30$ , strengthening the suggestion that something special occurs there. Most remarkable are the curves for  $h = 3$  and  $h = 4$ . The latter exhibits two peaks, one on each side of the  $n \approx 30$  region, with a dip in the middle resembling those for heights two and three. The  $h = 3$  curve, which asymptotically is supposed to rise to unity, instead descends so precipitously after  $n = 7$  that for  $25 \leq n \leq 33$  the fraction of posets of height 3 falls below that of height 6, decreasing to almost  $1/50$  at its minimum near  $n = 30$ . Not until  $n \approx 50$  does  $h = 3$  meet and surpass  $h = 4$ .

In the asymptotic regime, all the height-fractions except that of height 3 should decay to zero, with height 2 decaying the most slowly. Our results are broadly consistent with this expectation, although they do not yet reveal any obvious sign of decrease for height 2.

Figure 11: Measured heights of posets with  $n \leq 85$ .

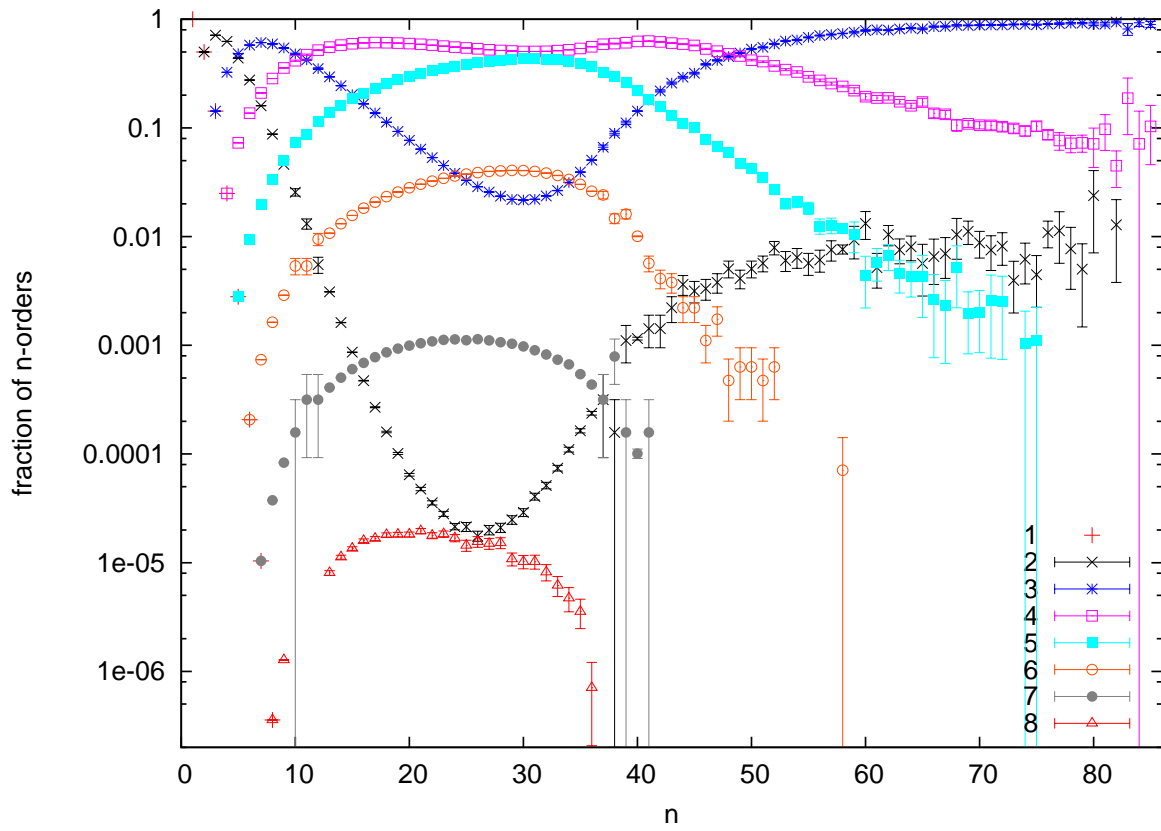


Figure 12: Same as Figure 11, in logscale.

In addition to plotting the full histogram of height as a function of  $n$ , it is interesting to examine the mean height vs.  $n$ , as depicted in Figure 13.

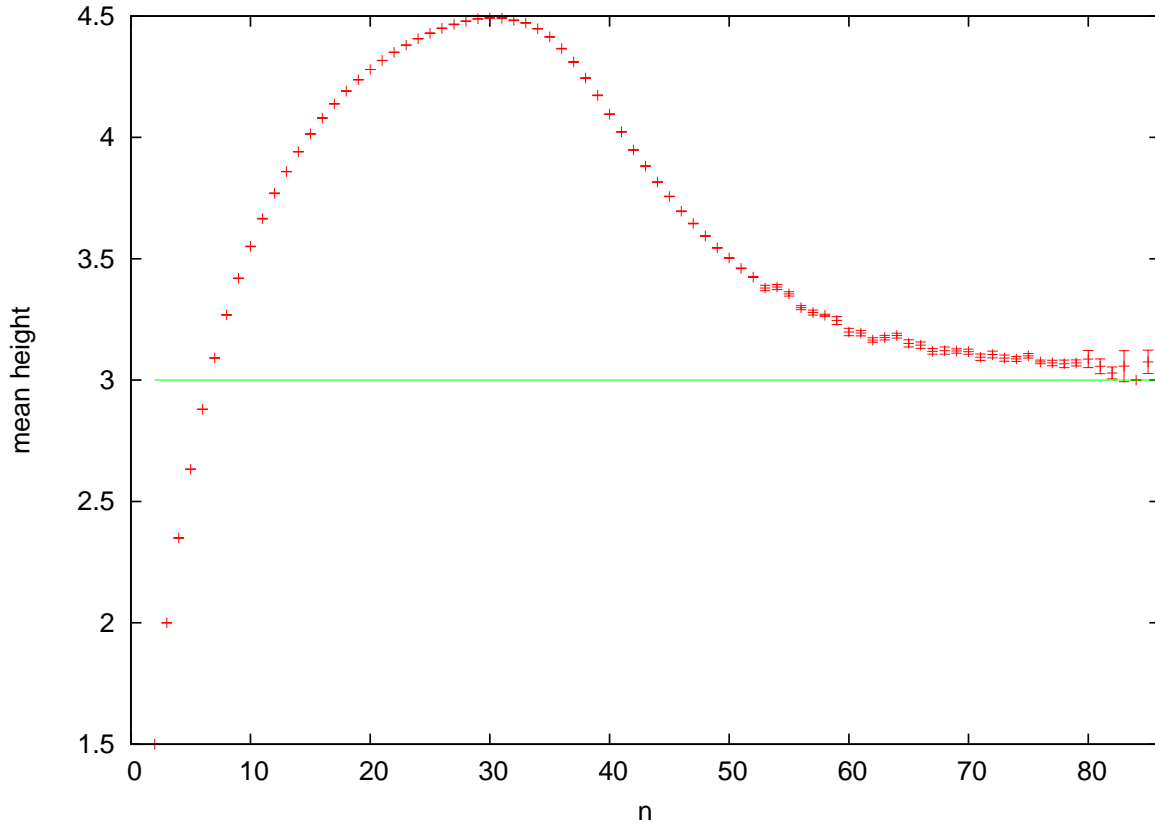


Figure 13: Mean height as a function of  $n$ , compared against the asymptotic value 3.

## 6.2 Connectivity of non-adjacent layers

The KR theorem of section 2 informs us that asymptotically almost every  $n$ -order belongs to the three-layer class of posets, and as such fulfills conditions (1) and (2) given just above the theorem. To examine the onset of this feature, we define a characteristic function  $\chi$  which takes the value 1 when conditions (1) and (2) are satisfied for the partitioning of the poset into levels,<sup>5</sup> and is zero otherwise. The fraction of such “layered” posets is depicted in Figure 14. As with the relative abundances of  $h = 3$  and  $h = 4$ , the layered posets do not surpass the unlayered ones until about  $n = 55$ .

A related condition, which is strictly stronger in the case of height 3 posets, is to demand that each

---

<sup>5</sup>For computational convenience, we have used here levels as proxies for layers. For this partitioning, condition (1) holds trivially.

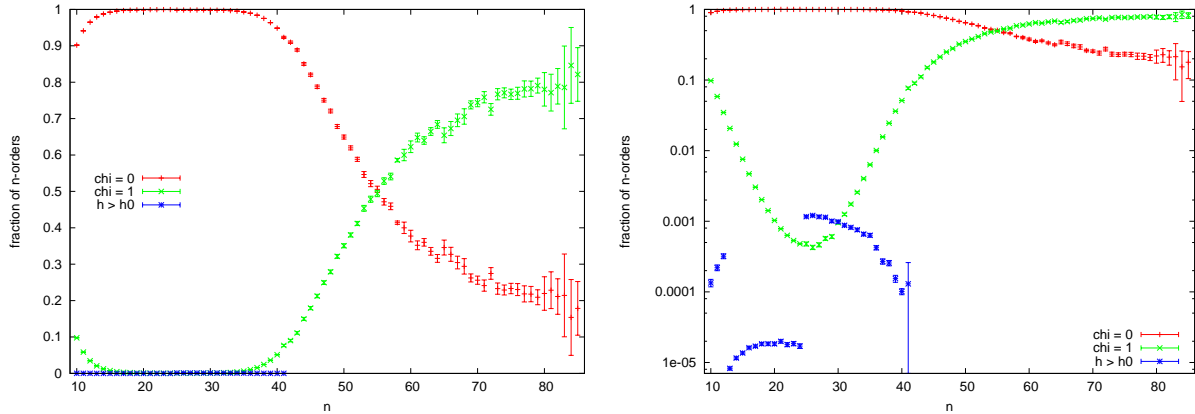


Figure 14: Fraction of posets whose levels do ( $\chi = 1$ ) and do not ( $\chi = 0$ ) satisfy condition (2) of Section 2. Here, to speed the analysis, if the number of levels of the poset exceeds  $h_0 = 7$  (for  $13 \leq n \leq 24$ ) or 6 (otherwise) we abandon the check of that poset. The plot on the right is in logscale.

of the minimal elements be related to each of the maximal elements. We do not check for this, since the property of being layered is not yet satisfied by more than around 4/5 of the 85-orders.

### 6.3 Cardinality of middle layer

We now consider the cardinality of the middle layer. Although it is not straightforward to determine whether a given poset has a layered structure in the sense of Sec. 2, it is easy to compute its decomposition into levels. Asymptotically, we expect level 2 to coincide with layer 2. As an indication of how well the quantitative bounds on layer size in the KR theorem are being satisfied, we plot, in Fig. 15, histograms of the cardinality of level 2 (divided by  $n$ ) for  $n = 72, 73, 76,$  and  $79$ , restricted to the posets of height 3. As expected, the curves (which evidently differ little from each other) are strongly peaked at  $n/2$ , with a width of less than 0.1 and a long tail that extends toward zero. This is consistent with what one would expect from the Kleitman-Rothschild theorem for the cardinality of layer 2.

### 6.4 Time asymmetry

Define the time reverse of a poset  $P$  as a poset  $P'$  which is identical to  $P$  except that the direction of each relation is reversed:  $x \prec y$  in  $P'$  iff  $y \prec x$  in  $P$ . The version of the KR theorem we have quoted above, implies that a typical  $n$ -order will be almost perfectly time-symmetric for  $n \gg 1$ . However, we have argued that our weighting by natural labellings is liable to invalidate this sort of conclusion. Indeed, an unconstrained division of elements between the the top and bottom layers would imply a significant amount of asymmetry, even as  $n \rightarrow \infty$ . In Fig. 16 we examine the situation for  $n = 58$ , by measuring

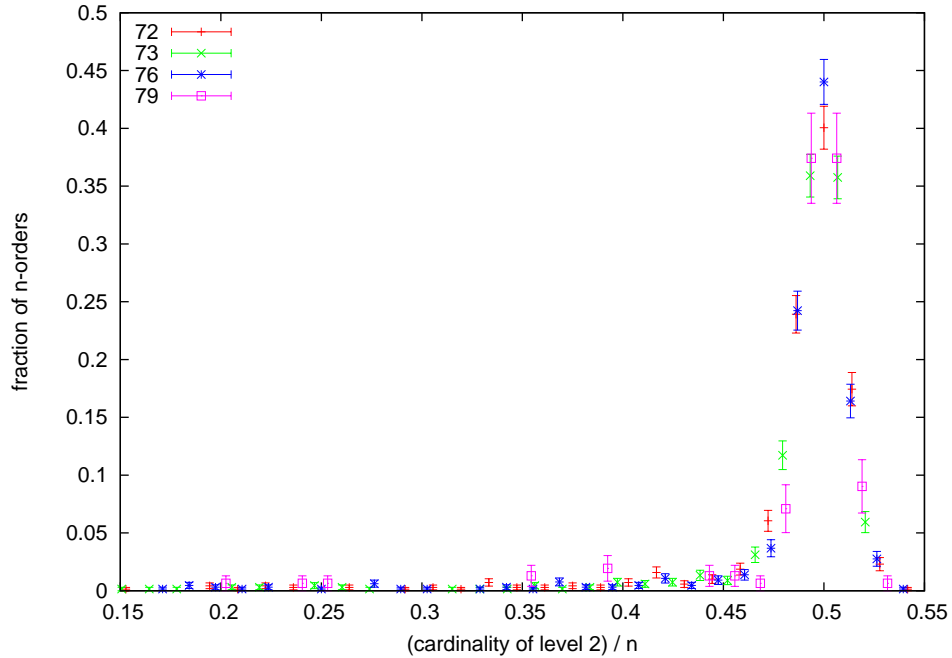


Figure 15: Histograms for the cardinality of level 2 for  $n = 72, 73, 76,$  and  $79$ , restricted to the posets of height 3.

a histogram of the number of minimal elements  $|\min|$ , the number of maximal elements  $|\max|$ , and the difference  $|\max| - |\min|$ . As they must, the histograms of  $|\min|$  and  $|\max|$  match each other (to within the estimated errors). But we notice that the cardinalities of the minimal and maximal layers are more likely to differ by  $\approx 17$  than by smaller or bigger values. In this sense most naturally labeled 58-orders exhibit a substantial time asymmetry, exceeding what one might have expected from the naive KR bounds. The same sort of asymmetry persists for other values of  $n$  as well.

Interestingly, a similar asymmetry was found in a generalization of the uniform model of random partial orders in which the ordering fraction  $r$  is held fixed [20].

## 6.5 Ordering fraction

The ordering fraction  $r$  of a poset is by definition the number  $R$  of pairs of related elements  $x \prec y$  divided by  $\binom{n}{2}$ . As described earlier in connection with the KR theorem, we expect — for naturally labeled orders — that  $r$  asymptotically will be distributed between  $1/4$  and  $3/8$  with a square-root-divergent peak at  $r = 3/8$ .

Figure 17 presents a histogram of  $r$  for  $n = 58$ . Evidently, it is nicely consistent with these expectations. The peak at  $r = 3/8 = 0.375$  is present, and the cutoff at  $r = 1/4$  is also observed. Except for

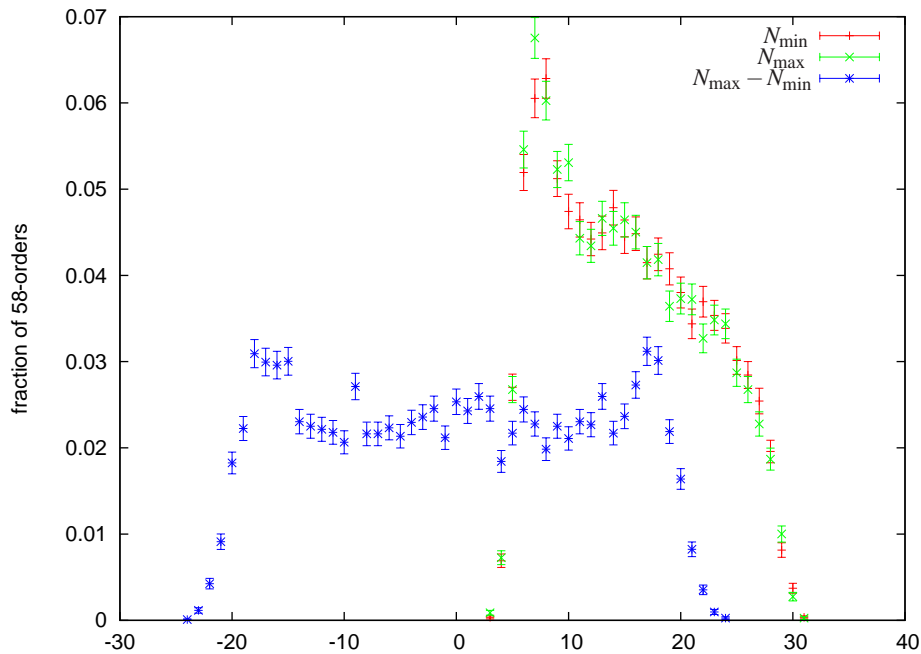


Figure 16: Histograms of the number of minimal and maximal elements, and their difference, for posets of 58 elements.

the fact that the histogram extends some way to the right of the peak, the agreement is surprisingly good, considering that a large number of posets of height 4 are still present at  $n = 58$ , as we saw above.

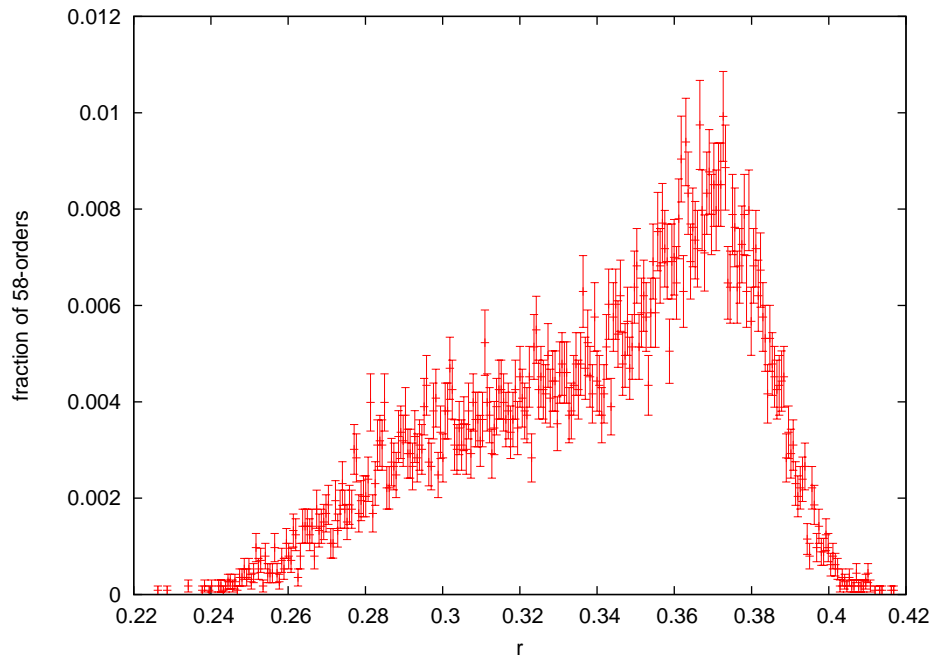
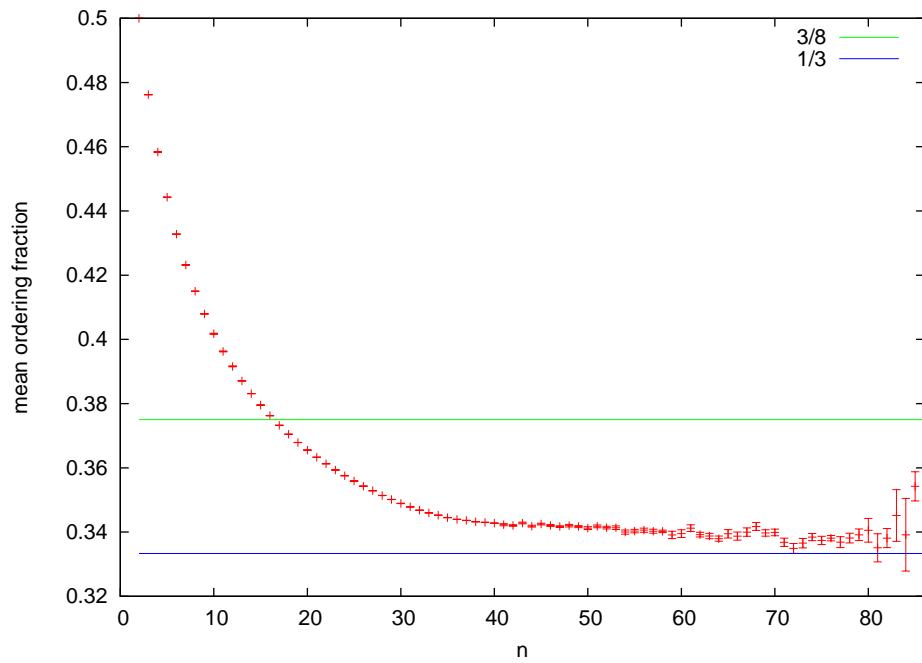
After 3-layer orders (or as a special case thereof), 2-layer or “bipartite” orders are expected to be next most abundant for large  $n$ . A typical bipartite order (one with both layers of size  $\approx n/2$ , such that each element of one layer is related to approximately  $n/4$  elements of the opposite layer) has  $r \approx 1/4$ , furnishing in effect the lower end of the 3-layer histogram. Once again, this is quite compatible with what one observes in Figure 17 in the neighborhood of  $r = 0.25$ .

To get additional feel for how  $r$  varies with  $n$ , we computed its expectation value, as shown in Figure 18. It seems evident that the mean is converging to something very close to the expected<sup>6</sup> value of  $1/3$ , and not to the “unlabeled KR” value of  $3/8$ .

## 7 Conclusions

Thanks to the groundbreaking results of Kleitman and Rothschild the asymptotic structure and enumeration of the finite partial orders are fairly well understood. However, almost 40 years since the publication

<sup>6</sup>“expected” but not “predicted”, since we understood the significance of natural vs. arbitrary labellings only after seeing this curve!

Figure 17: Histogram of ordering fraction  $r$  for  $n = 58$ .Figure 18: Plot of mean ordering fraction  $\langle r \rangle$  versus  $n$ .

of their main results, relatively little is known about the onset of the asymptotic regime, i.e., the poset size at which their results become relevant. While small posets can be generated exhaustively on a computer, the number of  $n$ -orders grows so rapidly with  $n$  that one cannot access the asymptotic, KR regime in this way.

The Markov chain algorithm presented herein opens a new window onto this question by sampling uniformly from the set of naturally labeled partial orders. We have used it to explore the structure of a “typical” poset up to  $n = 85$ . Although we still do not reach the deep asymptotic regime in this way, our results are consistent with a monotonic approach to asymptopia which begins around  $n = 45$  and is in full swing by  $n = 80$ . It seems likely from our data that this trend simply continues until it reaches substantial completion well past  $n = 100$ . Our simulations also reveal the presence of an interesting intermediate regime for  $n < 50$ , which is quite different from the asymptotic one, and whose best characterization remains to be understood.

Even though our algorithm allows uniform sampling of partial orders which are much larger than have been considered previously, one would like to be able to simulate still larger posets which are deep within the asymptotic regime. The construction of efficient algorithms, however, is hampered by the constraint of transitivity, which entails complicated dependencies among the defining relations  $x \prec y$ . One could circumvent this difficulty by identifying a set of simple, independent variables in terms of which the partial order could be defined, however we are not aware of any such representation of (generic) partial orders. To bypass the problems arising from the transitivity constraint, one might try to devise ‘cluster algorithms’ analogous to the Wolff algorithm for spin systems [21], which could change a large number of relations in a single move, while still maintaining transitivity. An alternative approach would be to drop transitivity and expand the sample space from  $\Omega_n$  to the set of all directed acyclic graphs. One could then impose Boltzmann weights which would keep the violations of transitivity small, or alternatively which would compensate for the overcounting resulting from failing to take a transitive closure.<sup>7</sup> The latter approach is currently being pursued [22]. Preliminary results for  $n < 55$  are in good agreement with the results reported above. In particular, the dip in the profiles for  $h \leq 4$  appearing in Figures 11 and 12 seems to be reproduced with high precision.

Throughout we have considered the set of naturally labeled partial orders. This choice was largely for convenience. Labeled posets are conveniently represented on a computer by their adjacency matrices, without any need to search for isomorphisms between different labellings. The choice is also convenient

---

<sup>7</sup>The observables would still be measured on the transitive closure of the directed graph, its “projection down to  $\Omega_n$ ”.

because one can easily take advantage of the CausalSets Toolkit within the Cactus HPC framework, which currently assumes natural labellings throughout.

We conclude with some questions concerning the possible relevance of posets to the still unsolved mystery surrounding the so-called arrow of time. If all the known laws of physics are invariant under reversal of the direction of time, from whence comes the extreme time-asymmetry that we observe? Locally finite posets in which the partial ordering is interpreted temporally (and which are called in that context causal sets) have been proposed as the deeper physical structure from which spacetime geometry emerges, and with discreteness comes a well-defined “counting entropy”. Could it be this entropy, rather than the kind of low entropy initial conditions on matter, radiation and event horizons, that are usually invoked, which will account for the arrow of time? Could time-asymmetric universes simply be much more plentiful than time symmetric ones, because time-asymmetric posets are more plentiful? A hint of this comes from the asymmetry observed in Sec. 6.4, but it’s doubtful that simple counting could by itself suffice to explain the observed degree of asymmetry in the cosmos. But perhaps in conjunction with other dynamical constraints, like those in [20], it could be a part of the answer.

**Acknowledgments** We are grateful to a number of people for comments and suggestions, including Samo Jordan, Lisa Glaser, Andrzej Gorlich, Denjoe O’Connor, Jeff Remmel, Orest Bucicovschi, and Graham Brightwell.

This work was funded by a grant from the Foundational Questions Institute (FQXi) Fund on the basis of proposal FQXi-RFP3-1018. This work was also supported in part under an agreement with Theiss Research and funded by a grant from the FQXI Fund on the basis of proposal FQXi-RFP3-1346 to the Foundational Questions Institute. The FQXI Fund is a donor advised fund of the Silicon Valley Community Foundation. This research was also supported in part by NSERC through grant RGPIN-418709-2012. This research was additionally supported in part by Perimeter Institute for Theoretical Physics. Research at Perimeter Institute is supported by the Government of Canada through Industry Canada and by the Province of Ontario through the Ministry of Research and Innovation. JH also receives support from EPSRC grant *DIQIP* and ERC grant *NLST*. This material is based in part upon work supported by DARPA under Award No. N66001-15-1-4064. Any opinions, findings, and conclusions or recommendations expressed in this publication are those of the authors and do not necessarily reflect the views of DARPA. This work used the Extreme Science and Engineering Discovery Environment (XSEDE), which is supported by National Science Foundation grant number ACI-1053575.

We thank Yaakoub El Khamra for his encouragement and assistance with profiling our code on Lonestar ([www.tacc.utexas.edu/resources/hpc/lonestar](http://www.tacc.utexas.edu/resources/hpc/lonestar)). Early trials were conducted on the HPC cluster at the Raman Research Institute.

## A Appendix

We here crudely estimate the number of naturally labeled 3-layer orders with layer sizes  $n_1, n_2, n_3$ .

Assume (as will almost always be true) that the poset is asymmetric (automorphism free), and for convenience let its elements be distinguishable. The number of ways to fill in the links between adjacent layers is

$$2^{n_1 n_2 + n_2 n_3} = 2^{(n_1 + n_3) n_2} = 2^{n_2 (n - n_2)}.$$

However, permuting the elements within any single layer produces a different set of links, but an isomorphic poset. Compensating for this over counting yields, for unlabeled posets,

$$\frac{2^{n_2 (n - n_2)}}{n_1! n_2! n_3!}.$$

Now let  $L(a, b)$  be the average number of natural labellings of a bipartite order with layers of size  $a$  and  $b$ . From [23] comes the estimate

$$L(a, b) = c a! b!,$$

where  $c = c(a, b)$  depends on  $a$  and  $b$ , but goes over to the constant  $\eta = 3.4627\dots$  as  $n \rightarrow \infty$  (and is typically smaller than that for finite  $n$ ). Thus we estimate

$$c(n_1, n_2) c(n_2, n_3) n_2! 2^{n_2 (n - n_2)}$$

naturally labeled orders with layer-sizes  $n_1, n_2, n_3$ , where asymptotically  $c = \eta$ .

The exponential factor peaks sharply at a middle-layer size of  $n_2 = n/2$ , and asymptotically dominates everything else. What remains is then independent of  $n_1$  and  $n_3$ , to the extent that  $c$  and  $n_2!$  can be treated as constant.

## References

- [1] G. Brinkmann and B. D. McKay, “Posets on up to 16 points,” *Order*, vol. 19, pp. 147–179, 2002.
- [2] D. Kleitman and B. Rothschild, “The number of finite topologies,” *Proc. Amer. Math. Society*, vol. 25, pp. 276–282, 1970.
- [3] D. P. Rideout and R. D. Sorkin, “Classical sequential growth dynamics for causal sets,” *Phys. Rev. D*, vol. 61, p. 024002, 2000. (e-print arXiv: gr-qc/9904062).

- [4] D. P. Rideout, *Dynamics of Causal Sets*. PhD thesis, Syracuse University, May 2001. (e-print arXiv: gr-qc/0212064).
- [5] S. Surya, “Evidence for a Phase Transition in 2D Causal Set Quantum Gravity,” *Class.Quant.Grav.*, vol. 29, p. 132001, 2012. (e-print arXiv: 1110.6244 [gr-qc]).
- [6] L. Bombelli, J. Lee, D. Meyer, and R. D. Sorkin, “Space-time as a causal set,” *Physical Review Letters*, vol. 59, pp. 521–524, 1987.
- [7] D. M. Benincasa and F. Dowker, “Scalar curvature of a causal set,” *Phys.Rev.Lett*, vol. 104, no. 181301, 2010. (e-print arXiv: 1001.2725).
- [8] G. Brightwell, “Models of random partial orders,” in *Surveys in combinatorics* (K. Walker, ed.), vol. 187 of *London Math. Soc. Lecture Note Ser.*, pp. 53–83, Cambridge: Cambridge University Press, 1993.
- [9] G. Brightwell, H. F. Dowker, R. S. Garcia, J. Henson, and R. D. Sorkin, “General covariance and the “problem of time” in a discrete cosmology,” in *Proceedings of the Alternative Natural Philosophy Association meeting*, August 16–21 2001. (e-print arXiv: gr-qc/0202097).
- [10] G. Brightwell, H. F. Dowker, R. S. Garcia, J. Henson, and R. D. Sorkin, ““Observables” in causal set cosmology,” *Phys. Rev. D*, vol. 67, no. 084031, 2003. (e-print arXiv: gr-qc/0210061).
- [11] J. Ambjorn, A. Goerlich, J. Jurkiewicz, and R. Loll, “Quantum Gravity via Causal Dynamical Triangulations,” in *Handbook of Spacetime* (A. Ashtekar and V. Petkov, eds.), Springer Verlag, 2014. (e-print arXiv: 1302.2173).
- [12] M. El-Zahar and N. Sauer, “Asymptotic enumeration of 2-dimensional posets,” *Order*, vol. 5, p. 239, 1988.
- [13] P. Winkler, “Random orders of dimension 2,” *Order*, vol. 7, p. 329, 1991.
- [14] M. E. J. Newman and G. T. Barkema, *Monte Carlo Methods in Statistical Physics*. Oxford University Press, 2007.
- [15] T. Goodale, G. Allen, G. Lanfermann, J. Massó, T. Radke, E. Seidel, and J. Shalf, “The Cactus framework and toolkit: Design and applications,” in *Vector and Parallel Processing — VECPAR 2002, 5th International Conference*, (Berlin), pp. 197–227, Springer, 2003.
- [16] G. Allen, T. Goodale, F. Löffler, D. Rideout, E. Schnetter, and E. Seidel, “Component specification in the Cactus framework: The Cactus configuration language,” in *2010 Workshop on Component-Based High Performance Computing (CBHPC 2010)*, 2010. (e-print arXiv: 1009.1341 [cs.DC]).
- [17] P. L’Ecuyer, “Tables of maximally equidistributed combined LFSR generators,” *Mathematics of Computation*, vol. 68, no. 225, pp. 261–269, 1999.
- [18] M. G. et al, *GNU Scientific Library Reference Manual*. 3rd ed. ISBN 0954612078.
- [19] R. D. Sorkin, “Catalog of posets of 9 or fewer elements.”
- [20] D. Dhar, “Entropy and phase transitions in partially ordered sets,” *J. Math. Phys.*, vol. 19, pp. 1711–1713, August 1978.
- [21] W. Krauth, “Cluster Monte Carlo algorithms,” Nov. 2003. (e-print arXiv: cond-mat/0311623).
- [22] M. Roy and S. Surya Work in progress.
- [23] G. Brightwell, H. J. Prömel, and A. Steger, “The average number of linear extensions of a partial order,” *Journal of Combinatorial Theory, Series A*, vol. 73, pp. 193–206, 1996.